"© 2022 IEEE. Personal use of this material is permitted. Permission from IEEE must be obtained for all other uses, in any current or future media, including reprinting/republishing this material for advertising or promotional purposes, creating new collective works, for resale or redistribution to servers or lists, or reuse of any copyrighted component of this work in other works."

Detection and Estimation of Cognitive Conflict During Physical Human-Robot Collaboration

Stefano Aldini[1], Avinash K. Singh[2], Daniel Leong[2], Yu-Kai Wang[2], Marc G. Carmichael[1], Dikai Liu[1] and Chin-Teng Lin[2]

***Abstract*—Robots for physical Human-Robot Collaboration (pHRC) often need to adapt their admittance and how they operate due to several factors. As the admittance of the system becomes variable throughout the workspace, it is not always straightforward for the operator to predict the robot's behaviour. Previous work demonstrated that cognitive conflicts can be detected during one-dimensional tasks. This work assesses whether cognitive conflicts can also be detected during 2D tasks in pHRC and a classification problem is formulated. Different robot admittance profiles anticipating the stimulus translated into different levels of cognitive conflict. Several commonly used classification algorithms for EEG signals were evaluated to classify different levels of cognitive conflict. Results demonstrate that cognitive conflict level is lower when the admittance smoothly decreases before unexpected events when compared to conditions in which the admittance abruptly decreases before the stimulus. Among the classification algorithms, Convolutional Neural Network has shown the best results to classify different levels of cognitive conflict. Results suggest the feasibility of adaptive approaches for future pHRC control systems that close the loop on users through EEG signals. The detected human cognitive state can also be used to assess and improve the predictability of Human-Robot teams in various pHRC applications.**

I. INTRODUCTION

Physical Human-Robot Interaction (pHRI) describes a scenario with a human in physical contact with a robot. Physical Human-Robot Collaboration (pHRC) defines a more specific scope, in which a human and a robot are in direct physical contact (or through a rigid body) and voluntarily exchanging forces to perform a common task. During the interaction, the human operator is always fully or partially in control of the human-robot system. Examples of robots for pHRC include a wearable robot for holding and lifting tasks [1] a robot for assembly tasks [2] and a robot to rehabilitate the hand [3]. Fig. 1a shows an example of a system for pHRC, with a human operator and a robot during a collaborative task [4].

In pHRC, the human and robot mostly base their interaction on the force exchange. Controls such as impedance- or admittance-based controllers are the most common ones in the field [6]. Both impedance and admittance are often used in pHRC as a way to guide the operator through the robot workspace, and to encourage or discourage some direction of motions. For example, if a resistive force is introduced along a specific direction of motion, the robot will present a lower admittance in that same direction. A lower admittance can be used to guide the robot operator away from undesirable configurations such as singularities and self-collisions. A lower admittance means that the operator has to exert higher forces to maintain a given velocity. This usually discourages the operator to move towards areas or configurations with lower admittance.

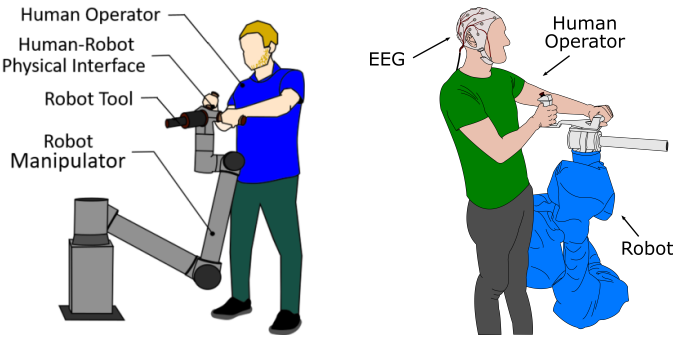

(a) Example of pHRC (b) Cognitive state in the loop

Fig. 1: (a) A pHRC application, with an operator physically controlling a robot [5]. (b) An operator controlling a manipulator during a pHRC application, while wearing an EEG device.

In many applications, other strategies are implemented in conjunction with the main control loop, such as singularity and collision avoidance and variable assistive paradigms ([7], [8], [9], [10]). Therefore, the resulting robot motions not only depend on the interaction force with the operator, but also on the combined result of the implemented strategies. As a consequence, the human operator often feels a variable admittance throughout the robot workspace. Due to the resulting complexity introduced by the implemented control strategies, the control gains are often empirically adjusted, along with the system resistance towards specific motions or configurations. Usually, the aim is to improve features such as the system smoothness and intuitiveness. Since there is generally no feedback to the user about the varying admittance other than through the force interaction itself, it has an impact on the predictability of the human-robot interaction.

A recent work by Maurice et al. suggested that when manipulating complex objects, humans try to increase the predictability of the task [11]. People constantly try to predict the outcomes of tasks that they are performing [12]. This ability is the result of past experiences. In pHRC, the relationship

[1]Stefano Aldini, Marc Carmichael and Dikai Liu are with the Centre for Autonomous Systems, Faculty of Engineering and Information Technology, University of Technology Sydney, 81 Broadway, Ultimo NSW 2007, Australia stefano.aldini@uts.edu.au

[2]Avinash K Singh, Daniel Leong, Yu-Kai Wang and Chin-Teng Lin are with the Centre for Artificial Intelligence, School of Computer Science, Faculty of Engineering and Information Technology, University of Technology Sydney, 81 Broadway, Ultimo NSW 2007, Australia avinash.singh@uts.edu.au

between the design of the interaction and the task predictability is not clear. Consequently, a rigorous mathematical approach for designing and tuning the control system is impossible.

In this paper, we investigate effective methods of detection and estimation of cognitive conflict in pHRC. A cognitive conflict is a cognitive state that can result from a prediction error. A resistive force was introduced to result in admittance that would generate different levels of cognitive conflict. Data were first processed to see whether cognitive conflicts can be identified and visualized. Further, we compare six different classifiers on the collected datasets, to see which algorithm presents better performances in detecting a cognitive conflict. This work represents a milestone towards closing the loop on the human cognitive state during pHRC applications (future work). In Section II, the authors provide the reader with background about cognitive conflict and related works in Human-Robot Interaction (HRI). In Section III, we first present the method that we implemented to evaluate the effect of an unexpected decrease of admittance on cognitive conflicts in the event-related potential (ERP) [13], with the relative results and discussion. In Section IV the classification problem and methods are presented with results. Section V addresses limitations of experiments and results and Section VI draws the conclusions of this work.

This paper is an extension of two conference papers, [5] and [14]. In [5], we presented some preliminary results about whether resistive forces can generate cognitive conflicts, with only four participants who performed experiment 1 (Exp1). In [14], we presented results for ten participants performing Exp1, with a focus on the processing pipeline, and provided a statistical analysis on the relevance of the results, without detailing the mechanical admittance between the human and the robot. The novel contributions presented in this work are the following:

- Extension of Exp1 to two dimensions (Exp2);
- Comparison of six classifiers for the detection and classification of cognitive conflicts, with the data collected from eleven participants while performing Exp1;
- Detailed insights on the design of the resistive forces and on the resulting mechanical admittance of the robot, to trigger and evaluate cognitive conflicts (in Section III-D).

II. COGNITIVE CONFLICT AND RELATED WORKS

Human internal models are the result of a cognitive process that simulates a task to predict its outcome [15]. A mismatch between internal models and reality causes a phenomenon called cognitive conflict [16]. For the sake of clarity, cognitive conflict is not necessarily related to the cognitive burden due to a complex task. The outcomes of a simple task can differ from what a person anticipated, causing a cognitive conflict.

A relationship between the cognitive conflict and a feature in the ERP was first found by Falkenstein et al. [17], using an electroencephalogram (EEG). Falkenstein et al. noticed a negative peak in the ERP which is known as error-related potential (ErrP) or error-related negativity (ERN) and caused by erroneous behaviour of tasks. Prediction error negativity (PEN) [18] is a specific type of ERN that has fundamental differences that were not seen before in other forms of negativity. PEN is invoked before completing the task, while other types of negativity are evoked once the task is finished. Moreover, PEN is evoked in tasks in which participants are actively involved in mobile brain/body imaging (MoBI) settings [19], while other negativities are evoked in tasks in which participants passively observe the erroneous behaviour. PEN is a novel form of bio-marker invoked at 50-250ms after the onset of a prediction error.

Recently, there has been interest in trying to integrate robot systems with Brain-Machine Interfaces (BMIs). Previous works tried to integrate the detection of cognitive conflict in human-robot interaction. Iturrate et al. [20], [21] performed an experiment in which participants were asked to judge whether a robot was performing an action correctly. They found negativity in the ERP around 400ms following an incorrect action and developed a reinforcement learning method to reduce the cognitive conflict. Penaloza et al. [22] used ERN invoked by observation of an unexpected action to trigger safety measures in a robot during a navigation task. More recently, Ehrlich et al. [23] detected ERN during human-robot social interaction and Salazar-Gomez et al. [24] used ERN while a human operator supervised a robot. Salazar-Gomez et al. also used reinforcement learning to close the loop on the robot control and reduce the cognitive conflict.

In all the above-mentioned works, the operator was not in physical contact with the robot. There are several issues related to the use of EEG for interactions that require active motor movements. Limb motions introduce artifacts and confounding factors that make the processing of brain signals more difficult [25]. By overcoming the effect of motor effects and confounding factors, we propose the use of PEN to increase the predictability of pHRC tasks and hence improve the physical human-robot interaction. In the future, robots will possibly adapt their behaviour depending on the cognitive state of the operator. In Fig. 1b, an operator is controlling a robot during a pHRC task, while their cognitive state is being estimated.

III. COGNITIVE CONFLICT IN THE EVENT RELATED POTENTIALS

A repetitive task creates human internal models that allow people to predict the outcome of the task. If the task has a different outcome than the predicted one (the internal models are proven wrong), a cognitive conflict should be invoked. This is the idea behind the implemented experiments. In this section, we demonstrate that the interaction dynamics can affect the cognitive state of the operator.

A. Experimental setup

The experimental setup for the experiments is similar to the one reported in [5]. The robot used in the experiments is the ANBOT [4]. To reduce potential artifacts and disturbances affecting the cognitive state, the task was initially designed to be as simple as possible, then extended to a more complex task. The motion was initially limited to one direction in experiment 1 (Exp1). Exp1 was then extended to a planar

task in experiment 2 (Exp2) to see whether the findings from the one-dimensional (1-D) case are also valid in a two-dimensional (2-D) scenario. The use of a 6-degrees-of-freedom arm is justified by the will of the authors to move this research towards a pHRC task involving free motions in the three-dimensional (3-D) space.

A 32-channels wireless EEG device named MOVE (Brain Product GmbH, Germany) is used to measure brain activity. The placement of the EEG electrodes is consistent with the 10-20 international system [26]. The contact impedance is maintained below $25k\Omega$ with a sampling rate of $500Hz$.

Data were collected from eleven healthy participants in Exp1, nine males and two females between 25 and 39 years of age. Only two participants (one male and one female) carried out Exp2. As mentioned above, the planar task is used to verify that the findings of Exp1 are valid for multi-dimensional tasks as well. This experiment follows the procedures approved by the UTS Human Research Ethics Committee with approval numbers ETH15-0038 and ETH18-2732. The experiments present a within-subject design, in which each participant performed four sets of 125 trials, resulting in 500 trials in total per participant, as detailed in Section III-B. In Fig. 2a a participant is shown while collaborating with the robot to perform the experiment.

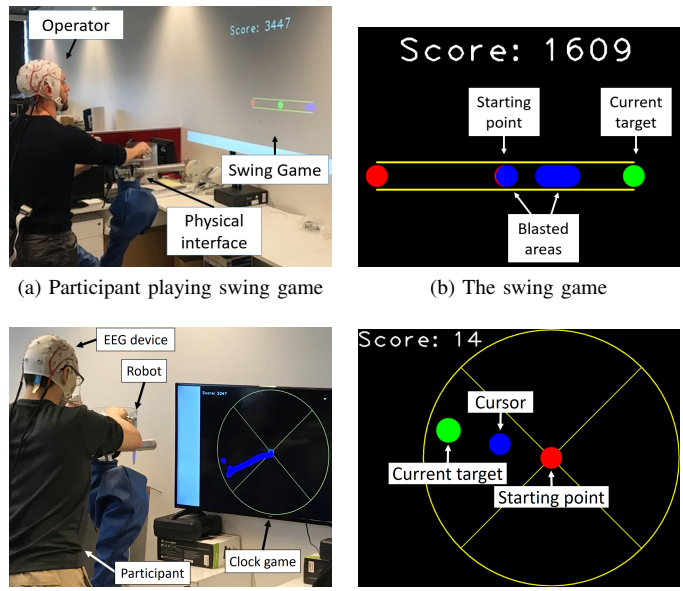

(a) Participant playing swing game (b) The swing game

(c) Participant playing clock game (d) The clock game

Fig. 2: (a) A participant performing the swing game [5]. (b) Layout of the swing game [5]. (c) A participant performing the clock game. (d) Layout of the clock game.

B. Task design

The "swing game" is a game implemented to create a repetitive 1-D task for Exp1. This task is extensively detailed in [5], but since the classification problem addressed in Section IV uses data collected with participants performing Exp1, a short description of the task is required in this paper. The layout is shown in Fig. 2b and is designed to be as simple as possible, to avoid giving too many cognitive stimuli to the operator. In Exp1, the operator can move the robot only horizontally, parallel to the wall where the task interface is projected.

The blue circle is the cursor, representing the point in the display the nozzle of the robot is aiming at. In the game, there are three potential targets: centre, left-end and right-end. The user is instructed to move the cursor to whichever target is turned green. The other targets will be red. To keep the participant slightly engaged and to ensure that both their hands are in contact with the robot, a blasting scenario was emulated: holding pressed only the trigger on the back handle of the end-effector would move the robot, and consequently the cursor, while holding pressed the trigger on the front handle would paint blue the area where the cursor is.

Each trial starts from the target in the centre. Once the cursor is placed on the starting point, one of the other targets is randomly turned from red to green. Having the target in the centre as the starting point ensures that the participant cannot anticipate the direction of motion to get to the next target. The participant has five seconds to reach the green target otherwise the trial is reset and the current target turns red, while the starting point becomes green, to inform the participant that they have to go back. If the operator reaches the target the robot will be locked in that position till the end of the trial, preventing the robot to move for that lapse of time.

The score displayed on the game layout is proportional to the blasted area and inversely proportional to the distance from the current target when the time for the trial is over. Its purpose is to keep the user slightly engaged in the game.

For the 2-D task, a game called the "clock game" was designed and implemented. In this case, the operator can move the robot end-effector on a plane parallel to the task display. The clock game is a 2-D extension of the swing game. As shown in Fig. 2d, the layout presents the starting point located at its centre, surrounded by twelve potential targets. In this game, only the current target (in green) is displayed on the screen, to reduce the number of visual inputs given to the participant. In Fig. 2c a participant is shown while performing the 2-D experiment.

C. PEN Stimulus

To produce a cognitive conflict, an unexpected event is integrated into the games as a stimulus. In Exp1, an invisible obstacle is placed halfway between the cursor and the target, with a probability of 40%. In Exp2, the invisible obstacle is an annular barrier placed halfway between the starting point and the target, to prevent the participant from moving around the obstacle to reach the target. This probability is a compromise between preventing participants from creating an internal model in which the obstacle is likely to be encountered and having enough trials to perform a statistical analysis. The trials with the unexpected event are randomised. When the cursor hits the obstacle the robot motions are locked and, consequently, the cursor cannot be moved to reach the target. The obstacle is invisible to the participant, resulting in a cognitive conflict: while the participant moves the cursor towards the current target, unexpectedly, their motion will be locked, preventing them from reaching it. The robot will not

move until the trial time is over, regardless of whether the operator reaches the obstacle or the target. Since the obstacle is invisible, a visual stimulus will not be introduced, and the cognitive load should only be affected by the haptic signal that the participant is constantly processing during the task.

D. Control system and admittance design

This section contains the description of the implemented control system necessary to understand how the pHRC is obtained in the two experiments. Some concepts were previously outlined in [5], for Exp1, but this paper provides novel insights on the design of the robot admittance that were not previously discussed. An admittance-based controller [27] is used to transform forces exerted by the operator on the handles into desired robot velocities in the Cartesian space. To avoid influencing the admittance of the robot by adding a singularity avoidance strategy, we limited the task to a portion of the robot workspace, in which the manipulator would always be in non-singular configurations. This guarantees that the Jacobian matrix is always invertible in the task workspace, without an active singularity avoidance algorithm, which would induce unintended resistive forces. The desired Cartesian velocities are calculated as follows:

$$\dot{x}_d = A(f_H + f_D - f_R) \tag{1}$$

With $\dot{x}_d$ being the vector of desired velocities of the robot end-effector in the Cartesian space, A the diagonal matrix containing the admittance gains, f_H the vector of interaction forces exchanged with the human operator, f_D a force vector that smoothens the velocities in the Cartesian space and f_R the resistive force introduced to assess the cognitive conflict. The admittance gains are set to $0.01m/sN$ for the linear components and $0.4rad/sN$ for the angular components. The force f_D is obtained by multiplying the actual Cartesian velocity of the robot end-effector, $\dot{x}_r$, by a diagonal matrix of gains acting as a damper, D. The linear components of D are set to $0.01Ns/m$, while its angular components are set to $1Ns/rad$. The block diagram of the control system is presented in Fig. 3.

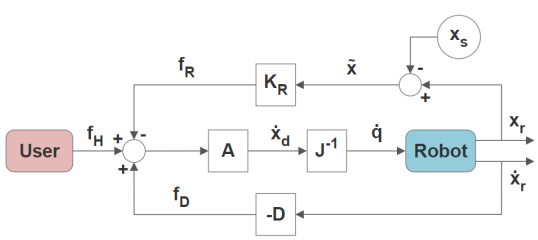

Fig. 3: The implemented admittance control [5].

For the purpose of the experiments, the directions and orientations in which the robot end-effector cannot move are limited using a basic P controller. This regulates the position of the end-effector at particular set points in those directions. With i symbolising the directions and orientations of the end-effector in Cartesian space, and $i = 1$ being the direction of motion in Exp1, the control system for the 1-D task can be summarized by:

$$\begin{cases} \dot{x}_d^i = A(f_H^i + f_D^i - f_R^i), & \text{if} \quad i = 1 \\ \dot{x}_d^i = K_P(x_d^i - x_r^i), & \text{if} \quad 2 \leq i \leq 6 \end{cases} \tag{2}$$

In Exp2, the top equation in (2) is valid for $i = 1, 2$, the two active directions in the planar task. The proportional gains for the position control are set to $K_P = 0.2$, expressed in N/m for the locked directions and N/rad for the locked orientations. The actual Cartesian position of the i-th direction is x_r^i, while x_d^i is the desired Cartesian position.

The resistive force f_R is designed to resist the motion as a compressed spring and it is used to shape the admittance in the implemented experiments. To study the effect of the admittance dynamics on the cognitive state of the operator, three different cases were analysed. Above, in (1), we defined A as a diagonal matrix containing the admittance gains of the system. A represents the admittance of the system when considering the sum of forces in the Cartesian space. The operator is however only responsible for f_H and the admittance that they experience is $A^* = \dot{x}_d/f_H$. In the experiments, we consider three admittance dynamics:

1) Admittance rapidly decreasing before an invisible obstacle;
2) Admittance slowly decreasing before an invisible obstacle;
3) Constant admittance or no invisible obstacle.

The decrease in the curves can be represented by their gradient. In the case of no invisible obstacle, the operator will expect a reduction of the admittance before the visible target, so that case does not produce any cognitive conflict, just like if there was no change in the admittance, therefore a zero-gradient curve. To analyse whether is the change in admittance that introduces a cognitive conflict rather than the presence of the invisible obstacle, we apply the same decrease of admittance before the visible targets. As we have two different gradients for the admittance in case of obstacles and we have the same two admittance gradients in case of no obstacle, we have a total of four conditions:

1) *Sudden-Normal* (Su-Nor): abrupt force, without obstacle or barrier;
2) *Sudden-Obstacle* (Su-Ob): abrupt force, with obstacle or barrier;
3) *Smooth-Normal* (Sm-Nor): smooth force, without obstacle or barrier;
4) *Smooth-Obstacle* (Sm-Ob): smooth force, with obstacle or barrier.

The *Normal* condition refers to trials without an obstacle, while the *Obstacle* one presents the invisible obstacle or barrier. To describe the nature of the decrease of the admittance, *Sudden* and *Smooth* are used. For example, a Sudden-Obstacle (Su-Ob) condition refers to trials with a sudden decrease of the admittance and an invisible obstacle or barrier. For the swing game, this translates in the four conditions shown in Fig. 4a.

The conditions represented in Fig. 4a can be mapped to the admittance gradients mentioned above. A Sudden-Obstacle corresponds to an admittance curve with a high gradient,

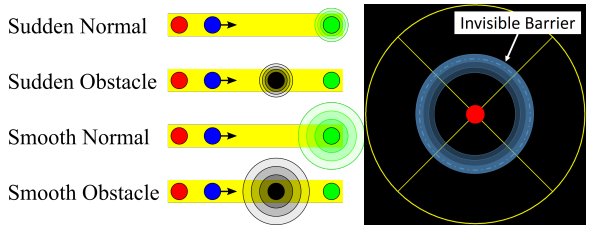

(a) 1-D conditions (b) 2-D barrier

Fig. 4: (a) The four conditions in the swing game. In this picture, the red circle is the starting point, the blue one is the cursor and the green one is the target. The black circle is the invisible obstacle. The circles around the target and obstacle represent the resistive force [5]. (b) Visual representation of the invisible barrier, in the 2–D scenario for the Obstacle condition.

while the Smooth-Obstacle corresponds to a curve with a low gradient. The zero-gradient curve corresponds to having no unexpected stimulus, so to Sudden-Normal and Smooth-Normal conditions. We remind the reader that to generate an unexpected scenario in the clock game, the obstacle has the form of a annular barrier (Fig. 4b), to avoid the participant moving around the obstacle to reach the target, with 2-dimensional movements involved.

To modulate the admittance and its gradient, the resistive force f_R is used. This force has first-order dynamics as a higher order would have naturally led to question what parameters are affecting the cognitive conflict the most. As this is the first attempt to detect cognitive conflicts in pHRC applications, tasks and forces are designed to be as simple as possible. The resistive force is designed to resist the motion as a compressed spring and is calculated using Hooke's Law:

$$f_R = K_R \tilde{x} \tag{3}$$

The stiffness gain is K_R and is multiplied by $\tilde{x}$, the difference between the position of the cursor and the onset position x_s of the resistive force. We define the position of the cursor in the game as x_p (the point in the display aimed by the nozzle of the ANBOT). The position where the motion of the robot is locked is x_t and it corresponds to the location of the target in case of Normal conditions and to the location of the invisible obstacle in case case of Obstacle conditions. With the cursor coming from the starting point, x_f is located before the target or the obstacle, so that the onset of the force would be located at $x_s = x_t - x_f$. Therefore, (3) becomes:

$$\begin{cases} f_R = 0, & \text{if} \quad x_p \leq x_s \\ f_R = K_R(x_p - (x_t - x_f)), & \text{if} \quad x_s \leq x_p \leq x_t \end{cases} \tag{4}$$

As mentioned above, when x_p reaches x_t, the robot motions are stopped. As the force is calculated with respect to the position of the cursor in the game, x_p and x_f are expressed in pixels. The conversion factor between pixels and the robot movements is $1px = 1.15mm$. The stiffness is set to $K_R = 0.5N/px$.

In Exp1 the targets are located $265px$ from the starting point, while the obstacles are 132 pixels from it. To experience an abrupt resistance, in the Sudden condition, x_f is located $20px$, or $2.3cm$, before the centre of the target or the obstacle. In case of a Smooth condition, x_f is positioned $80px$, or $9.2cm$, from the target or the obstacle. K_R and x_f are chosen with the specific purpose of having a clear difference in admittance between the different conditions. K_R is the same in all conditions, due to the fact that the cursor stops moving when the obstacle or target are reached and, together with the clear difference of x_f, the admittance results decreasing much quicker in case of the Sudden conditions.

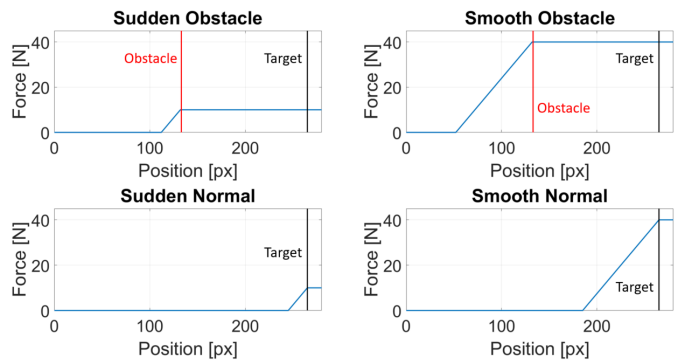

Fig. 5: The resistive force f_R for each condition, with respect to the cursor position x_p, in the 1-D scenario.

Fig. 5 shows f_R with respects to x_p, for the four conditions, in case of Exp1. With a black vertical line, the position of the target is reported. The target is visible for all the conditions. In case of Obstacle conditions, the location of the obstacle is reported with a red vertical line. The resistive force in case of Smooth condition builds up to a higher value, but it takes longer in terms of time. It can be noticed that the force starts increasing earlier in that case.

In case of Exp2, the resistive force is also calculated with (4) and with the same parameters specified above in this same section, but with the difference that f_R and $\tilde{x}$ have two components and K_R is a 2×2 diagonal matrix.

E. EEG signals pre-processing

The signal pre-processing for the ERP analysis is detailed in [14]. Cognitive conflict is represented by PEN, which is a negative deflection in the ERP happening around $50 - 250ms$ after the stimulus in the frontal area of the brain. Therefore, we focus on ERP at Fz, which is a mid-line frontal EEG channel. We used EEGLAB [28] on MATLAB R2018a (Mathworks Inc, USA). The raw signals are filtered using a 2Hz high-pass and a 50Hz low-pass finite impulse response (FIR) filter. Subsequently, the data is down-sampled to 250Hz. EEG channels with a too high noise-to-signal ratio and artifacts related to eye movement, muscle activity and other noise are rejected using artifact subspace reconstruction (ASR) [29].

Independent component analysis (ICA) [30] is then applied to the datasets, which are further filtered using an automatic EEG artifact detection algorithm with the help of ADJUST [31]. Dipoles of the ICs are evaluated and the ICs

with a residual variance greater than 15% are removed. Epochs are extracted from 500ms before the force stimulus is applied to the user to 1000ms after the stimulus. The force stimulus is represented by the onset of the resistive force and the extracted epochs are then divided by condition. A total of 5500 trials were collected with Exp1 from all the participants together and 1000 trials were collected with Exp2. They can all be divided into four sets, given the different conditions (Fig. 4a).

F. Results of ERP analysis

The ERP results for Exp1 presented here are similar to the ones presented in [14], as they only add one participant to the cohort. Understanding the data in terms of ERP is however critical to what addressed in Section IV, as the same data were used to formulate the classification problem. Epochs were extracted according to trial conditions and the ERP amplitudes were obtained. The ERP amplitudes shown in Fig. 6 are the results of the average between all the trials carried out by all participants. The bands around the curve represent the variance between different participants. The curves are sorted by condition and the zero of the x-axis (time [ms]) represents the time of the onset of the resistive force. In case of the Sudden-Obstacle condition (blue curve), around 200ms it can be noticed a negative deflection, which corresponds to PEN. Following the negativity, a positive peak appears around 350ms. That feature is associated with memory processing and is known as P300 [32]. We consider as a baseline the ERP amplitude in between -100ms and 0ms, which represent the cognitive state of the participant before the stimulus. For the other conditions, the ERP curves are comparable to that baseline. Since the same force as Sudden-Obstacle is applied before the target in the Sudden-Normal condition, it can be assumed that the only presence of an abrupt force is not enough to invoke PEN. In fact, in case of a visible target, the user can predict the presence of the force. Even if the two Normal conditions represent the case in which no PEN should be invoked, the plots of all four conditions are presented separately to highlight that the investigated EEG feature is not a result of the resistive force.

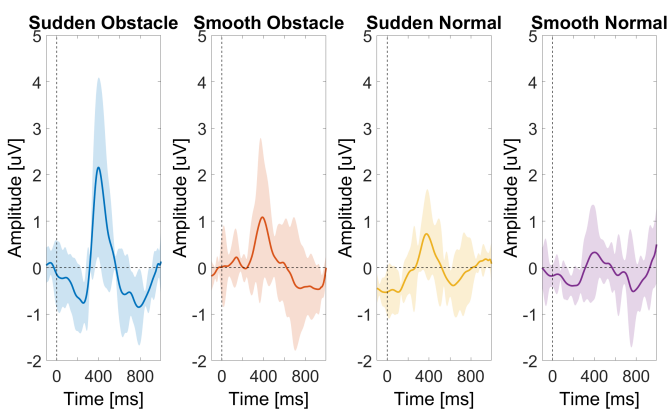

Fig. 6: Average of ERP amplitude for each condition, in Exp1. The zero-time corresponds to the onset of the resistive force..

When compared to the other conditions, Sudden-Obstacle presents a PEN amplitude that is higher (more negative) in 81.8% of the participants who performed Exp1. These results suggest that the way the admittance is designed to affect the cognitive state of the operator and that PEN can be used to estimate the predictability of the interaction. The condition Smooth-Obstacle does not present a negative deflection higher in magnitude when compared to the conditions with no invisible obstacle. In [14] details about the ERP results for Exp1 are presented for ten participants.

The ERP curves presented in Fig. 6 suggest that the resistive force modulates PEN. With a wider, smoother resistance around the obstacle, in Smooth-Obstacle conditions, the participant presented less cognitive conflict in terms of PEN amplitude (less negative). On the other hand, when an abrupt resistive force is applied, participants present more negative PEN, translating in a greater cognitive conflict. This means that abruptly interrupting the robot motion during a collaborative task without a visual feedback will likely lead to a cognitive conflict. On the other hand, applying wider and smoother resistive forces to avoid undesired areas of the workspace would decrease the level of cognitive conflict. It is hypothesised that this is a consequence of the operator being able to better anticipate the workspace dynamics when the robot starts resisting the motion sooner and more gently. The cognitive conflict resulting from the Sudden-Obstacle condition could be seen as the effect of the lack of an appropriate signal from the robot to communicate the presence of the obstacle.

Results of the 2-D scenario support the findings of the 1-D scenario, suggesting that the design of the interaction dynamics affects the cognitive state of the operator. Results are obtained processing and analysing data collected from two participants while using the clock game. The authors are aware that two participants do not represent a robust sample, especially for statistical analysis. In this work, the extension to the 2-D scenario has the purpose of verifying that the results from the 1-D task can be extended to multi-dimensional scenarios without losing validity. Fig. 7 presents the ERP amplitude for each condition as an average between the two participants. It can be noticed a higher PEN (more negative) in case of the condition Sudden-Obstacle, when compared to the other conditions. Negative deflections can be seen also in Smooth-Obstacle and Sudden-Normal, with peaks of $-1.17\mu V$ and $-0.95\mu V$ on average respectively, but not as negative as with Sudden-Obstacle conditions ($-1.86\mu V$). Adding complexity to the task in terms of motions does not seem to affect the ability of the processing pipeline to detect a cognitive conflict.

IV. DETECTION AND CLASSIFICATION OF COGNITIVE CONFLICT

In Section III it is demonstrated that a cognitive conflict can be found in the ERP for specific conditions. The data processing used for the ERP analysis and described in Section III-E, however, cannot be used for an online application. EEG data have a poor signal-to-noise ratio, and for online detection of a specific feature (future work), the data cannot go through complex and time-consuming processing. In Fig. 8 the implemented pipeline for the detection and classification of cognitive conflict is pictured from a high-level perspective.

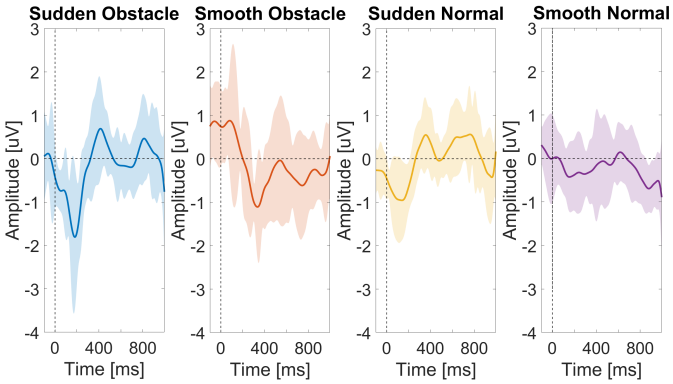

Fig. 7: Average of ERP amplitude for each condition, in Exp2. The zero-time corresponds to the onset of the resistive force.

There were 509 $\pm$ 44 number of trials on average for each participant, with 305 $\pm$ 19 for Normal condition, 107 $\pm$ 13 for Smooth-Obstacle condition and 98 $\pm$ 18 for Sudden-Obstacle condition. Each trial consists of dimension 32$\times$1200, where 32 is the number of EEG channels and 1200 is the number of sample points in each channel. For each participant, 60% of the trials were used to train the algorithm, 20% for validating and 20% for testing. The stratified sampling [33] has been used to divide data into training, validation, and testing. For the training set, the data was segmented by selecting the features, based on when the robot started applying a resistive force, before reaching the target or the obstacle. The selected interval is from -0.2s to 1s, where zero is the instant the robot starts resisting the human motion. The data was subsequently labelled, depending on the game condition and accordingly to the number of classes to identify with the classifiers. For the detection of cognitive conflict, the raw signals were band-pass filtered in the range of 1-15 Hz and resultant signals were used for classification. The band-pass filtered range corresponds to the δ, θ and α bands [34], since PEN is commonly associated with brain activity in the α and θ bands (4-13Hz) [35], [36].

A. Classifiers

To detect PEN, we have chosen the most popular classifiers for biomedical signals, with increasing level of space and computational complexity in order from linear, logarithmic, non-linear to artificial neural-network and deep learning corresponding respectively to the following algorithms. These classifiers are popular classification methods for ERPs. Lotte et al. present a detailed review of classification algorithms used for EEG-based BCIs [37]. The algorithms evaluated in this paper are the following:

- Linear Discriminant Analysis (LDA);
- Logistic Regression (LR);
- Support Vector Machine with a linear kernel (L-SVM)
- Support Vector Machine with a Radial Basis Function kernel (RBF-SVM)
- Multi-Layer Perceptron (MLP);
- Convolutional Neural Network (CNN).

The six classifiers used in the paper are here described. *Linear Discriminant Analysis* (LDA) is an algorithm widely used in BCI applications. LDA has very low computational requirements, which makes this algorithm a popular choice for online BCIs. LDA does not, however, perform well with complex non-linear EEG data without preprocessing, usually resulting in poor accuracy. *Logistic Regression* (LR) is a discriminative learning classifier. Results are usually more accurate than the ones obtained with LDA, but when data is sparse or high-dimensional LR can lead to overfitting issues. We used a Limited-memory Broyden-Fletcher-Goldfarb-Shanno (L-BFGS) solver for the LR. *Support Vector Machine* (SVM) algorithms can have different complexities depending on their decision boundaries. If the decision boundaries are linear, the corresponding SVM is defined as linear SVM (L-SVM). It is possible to have non-linear boundaries by using a kernel function. SVMs that use a Radial Basis Function kernels (RBF-SVM) are commonly used in BCI research. They have good generalisation properties, perform well with high-dimensional problems and are not sensitive to over-training. All those advantages come at the cost of execution speed. *Neural Networks* (NNs) consist of artificial neurons that can result in non-linear decision boundaries. NNs are very flexible and can approximate any continuous function, given they are provided with enough layers and nodes. We used a MultiLayer Perceptron (MLP). *Convolutional Neural Networks* (CNNs) [38] are deep NNs that use matrix convolution in at least one of their layer. They have the advantage of automatically optimizing weight parameters to minimise classification mistakes. This characteristic leads to a short preprocessing time.

For the RBF-SVM algorithm, we set γ = scale, with γ defining the influence of a single training trial. We used a MultiLayer Perceptron (MLP) with 100 hidden layers, learning rate α = 1 and the maximum iterations set to 1000, using Adam [39] optimizer with auto batch size selection. The other parameters were set as default, as mentioned in SciKit MLP. We have used the CNN model known as DeepConvNet [40]. It consists of four convolutional blocks and a classification block. The first convolutional block is specially designed to handle EEG inputs, and the other three are standard convolution ones followed by a softmax [41] classification with Adam [39] used as optimizer, with batch size in a range of 10 to 16, early stopping based on validation loss with patience of 20 epochs and a dropout rate for best performance chosen between 25% and 50%. The number of filters used in the CNN is 25, 50, 100, and 200 for each consecutive convolution layer, with the number of kernels equal to five. The parameters for all the classifiers compared in this paper have been set up before training and testing for all participants.

During Normal conditions, the operator can see the target and therefore there will not be a cognitive conflict regardless of the force condition. For that reason, the conditions Sudden-Normal and Smooth-Normal are considered as one class. We first addressed a two classes classification problem, with the class Sudden-Obstacle versus all the other conditions combined. The Sudden-Obstacle and Smooth-Obstacle conditions can, however, produce different magnitudes of PEN, resulting in different levels of cognitive conflict, with Sudden-Obstacle being higher (producing a more negative peak). Therefore

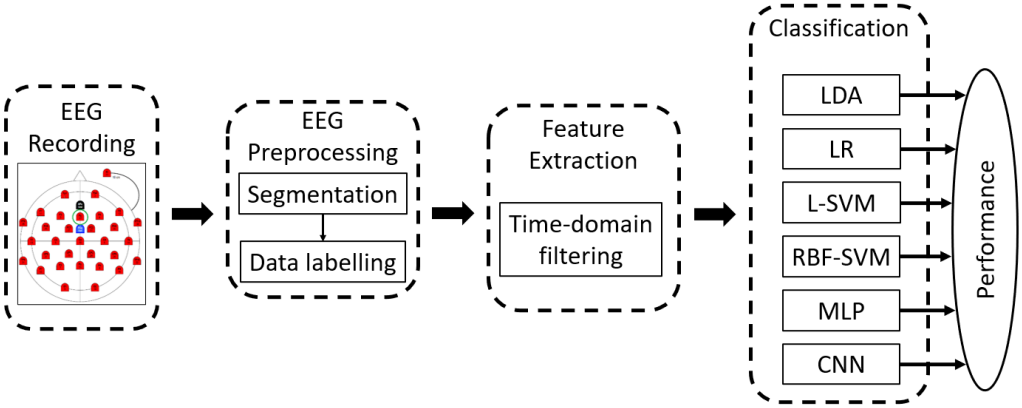

Fig. 8: The implemented pipeline for the classification of cognitive conflict through machine learning algorithms.

performances of the same algorithms were also tested in case of three classes: Sudden-Obstacle, Smooth-Obstacle and Normal. These would represent three different levels of cognitive conflict, that could be potentially used in applications that require a more precise estimation of the conflict.

To compare the results of different classifiers, we have evaluated overall accuracy, mean-squared error (MSE), computation time to predict (PT). We have an imbalance number of classes for different levels of cognitive conflict. Therefore, to better understand the performance of classification algorithms, we have also evaluated the precision (Pre), recall (Rec), and F1-score (F_1) for a targeted level of cognitive conflict (Sudden-Obstacle condition).

B. Classification Results

The performances of the six classifiers in case of two classes (Sudden-Obstacle versus all other conditions combined) are summarised in Table I. The accuracy is reported for all participants, with the mean and the standard deviation (SD). These results are the outcome of the testing phase of the classifiers. The accuracy of CNN is considerably higher than the one of the other classification algorithms. In the best case, with participant P11, the accuracy reached a level of 93.1%, with the CNN. The mean accuracy for CNN is 82.1% $\pm$ 5.2%, which is high considering that the data is only filtered in terms of frequency before being fed into the classifier.

In Fig. 9 the precision, recall and F_1-score are reported for the six classifiers. The values reported are the mean values across all participants. The CNN presents better parameters than the other classifiers.

Some applications might require a more precise estimation of the cognitive conflict. This leads to the necessity of the algorithm to detect multiple conflict levels. In our experiment, the condition Smooth-Obstacle is designed to have a reduced level of conflict. In case the classifier is required to detect three different classes, the accuracy is still acceptable for the CNN. The three classes are here representing the following conditions: Sudden-Obstacle, Smooth-Obstacle and Normal (Sudden-Normal and Smooth-Normal combined). In Table II, accuracy, MSE and prediction time are reported only for the CNN algorithm, as it performed better than the other

TABLE I: Resulting performances of the classifiers, in terms of accuracy (expressed in %), for each participant, in case of two classes: Sudden-Obstacle versus all the other conditions combined. In the last two rows, mean and standard deviation (SD) are reported.

		LDA	LR	L SVM	RBF SVM	MLP	CNN
Participant	P01	62.75	71.3	73.3	75.3	72.1	79.2
	P02	50.0	75.3	78.2	74.7	79.8	80.61
	P03	61.1	75.1	77.9	79.4	76.9	77.5
	P04	56.6	74.6	75.1	77.3	74.8	83.3
	P05	66.2	76.2	75.1	76.5	67.6	83.6
	P06	39.1	69.0	76.3	75.4	75.4	89.9
	P07	52.3	69.7	72.5	72.5	66.6	78.0
	P08	51.2	69.9	72.8	72.8	67.9	80.4
	P09	48.7	65.0	66.3	67.9	66.7	76.4
	P10	62.1	64.1	68.8	69.1	65.8	81.5
	P11	39.9	69.5	70.3	72.5	69.9	93.1
Mean		53.6	70.9	73.3	74.0	71.2	82.1
SD		9.1	4.1	3.7	3.4	4.8	5.2

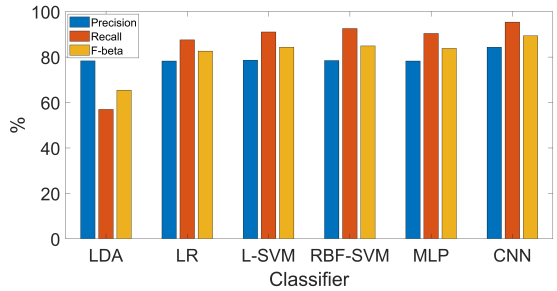

Fig. 9: Mean precision, recall and F_1-score with respect to the classifiers.

algorithms. In the case of three classes, the mean accuracy for LDA is 37.9%, for LR is 53.7%, for L-SVM is 54.1%, for RBF-SVM is 53.6% and for MLP is 46.9%. The mean accuracy for the CNN is 66.7% $\pm$ 10.2%, with a value of 91.1% for participant P11 as a best. This participant seems however to be an outlier, as most of the other participants present a much lower accuracy. The performance of the CNN

for three classes is reasonably lower than the ones relative to two classes. This is probably due to the fact that CNN is sensitive to the size of the data provided. As now we have three classes, the number of available training data for each class is smaller than in the case of classifying only two classes. We believe that with more data the performance of the CNN could improve significantly. The results still suggest that there is a difference between the condition Smooth Obstacle and the Normal conditions, even if it is not noticeable on the ERP plots. In a real-world application scenario, the class representing the condition Sudden-Obstacle is the most critical. Thus, the precision, recall and F_1-score (F_1) are also reported for each participant.

TABLE II: Accuracy (Acc) in %, Mean Square Error (MSE) and prediction time (PT), in seconds, in case a Convolutional Neural Network (CNN) is used to classify three classes: Sudden-Obstacle, Smooth-Obstacle and Normal. precision (Pre), recall (Rec) and F_1-score (F_1) are also reported for the Sudden-Obstacle class.

		Acc [%]	MSE	PT [s]	Sudden-Obstacle		
					Pre	Rec	F_1
Participant	**P01**	58.4	1.01	0.17	0.48	0.58	0.52
	P02	61.2	1.06	0.15	0.63	0.61	0.62
	P03	59.8	1.08	0.20	0.68	0.60	0.57
	P04	71.6	0.58	0.15	0.73	0.72	0.71
	P05	66.4	0.64	0.16	0.55	0.66	0.56
	P06	78.0	0.36	0.24	0.78	0.78	0.78
	P07	64.2	1.72	0.16	0.50	0.35	0.37
	P08	56.9	1.17	0.18	0.36	0.57	0.44
	P09	60.0	1.03	0.16	0.56	0.60	0.56
	P10	66.7	0.70	0.20	0.66	0.67	0.60
	P11	91.1	0.23	0.16	0.90	0.89	0.89
Mean		66.7	0.87	0.18	0.62	0.64	0.60
SD		10.2	0.42	0.03	0.15	0.14	0.15

If the CNN is used to detect the level of conflict and fed this information in a closed-loop system, the precision of the network has to be taken into account, allowing the system to react safely, also in the case of a false positive. Considering the mean values, the classifier might still be acceptable for three classes.

V. LIMITATIONS

This work contains limitations that should be addressed in future works. It would be interesting to also analyse the impact that previous experience with collaborative robots has to the cognitive conflict caused by a variable admittance. Only two participants performed the 2-D task and, ideally, it would be good to have a larger sample of participants to perform statistical analysis. The experiments in their current form are long, repetitive and tiring, and could lead to mental fatigue. Participants might also get physically fatigued, given that the experiment is performed in a standing pose. There might be potential artifacts that could not be removed with current methods. Since the stimulus is a force exchange that introduces many variables, both in the physical and mental domain. Confounding factors like stress, workload and fatigue could influence the results. Information from other physiological signals could help isolate those factors. For example, using electromyography(EMGs) could isolate muscular activity that usually introduces noise in the EEG signals.

The experiments scaled down the degrees of freedom of the tasks so that it would be easier to control events and conditions. This is a limited representation of the world. The objective is to prove the validity of the results also in the free space. We foresee the usage of the adopted CNN to detect the presence of PEN using the collected data as training sets. While specific events might be harder to identify in the absence of a clear task in the free space, the features identified in the EEG signals should be the same in case of a cognitive conflict.

The need for an EEG device to estimate the predictability of the system and eventually tune the control parameters inevitably adds complexity to the system. In industrial applications, wearing an EEG cap can often be an infeasible solution. This technology is however quickly improving. Hopefully, in the coming years, wireless dry EEG caps that present reliable signals will become available.

Another limitation of this work is the nature of the resistive force. As this is the first time PEN is assessed in pHRC scenarios, we opted for tasks and forces as simple as possible. Nowadays, in pHRC applications, those forces are usually more complex and do not present a first-order dynamics. As a result, the interaction is often perceived as more natural and resistive forces are more subtle. By using a proper classifier, it may still be possible to detect and estimate cognitive conflicts.

VI. CONCLUSION

Two experiments were performed to understand the effect of the robot admittance and resistive forces on the operator's cognitive conflict. The system admittance was designed to obtain four conditions that could be grouped into three classes of cognitive conflict. Results prove that an admittance that smoothly decreases, pushing the operator away from an undesired area of the workspace, helps the operator predict upcoming changes in the dynamics when compared to an abrupt admittance decrease. This is particularly relevant when considering the interaction dynamics of systems with multiple control strategies implemented, e.g. singularity and collision avoidance. Only in case of a sudden and unexpected reduction of admittance the operator presented PEN in the ERP plots, resulting in only two classes: cognitive conflict and no apparent cognitive conflict.

Six classifiers with different complexities were then compared to detect two and three classes of cognitive conflict. Results show that the CNN algorithm performed the best, with also good results in classifying three classes. This suggests that despite the results obtained in the ERPs there is a difference between the three classes. These results represent a further step into closing the loop on the cognitive state of the operator during pHRC applications.

Participants are here processing force signals and basing their interaction with the robot on internal models that were created based on experience. If the interaction between human and robot is generalised and the interaction itself is seen as a

task, human-human interactions could lead to similar results. Physical interactions between two humans could work in a similar way, which opens the question whether an unexpected reaction during a human-human interaction could trigger a cognitive conflict.

This opens new challenges and questions that need to be addressed to improve control systems in pHRC. Real-time estimation of the cognitive state of the operator could lead to control systems that adjust the parameters of the robot to increase the predictability of the physical interaction. Also, an objective measure of the predictability of a system could result in the development of improved pHRC paradigms.

ACKNOWLEDGMENT

This study is supported in part by the Australian Research Council (ARC) Discovery Project Grant [DP210101093].

REFERENCES

[1] T. Aida, H. Nozaki, and H. Kobayashi, "Development of muscle suit and application to factory laborers," in *2009 IEEE International Conference on Mechatronics and Automation, ICMA 2009*, 2009.

[2] A. Cherubini, R. Passama, A. Crosnier, A. Lasnier, and P. Fraisse, "Collaborative manufacturing with physical human-robot interaction," *Robotics and Computer-Integrated Manufacturing*, 2016.

[3] L. Masia, H. I. Krebs, P. Cappa, and N. Hogan, "Whole-arm rehabilitation following stroke: Hand module," in *Proceedings of the First IEEE/RAS-EMBS International Conference on Biomedical Robotics and Biomechatronics, 2006, BioRob 2006*, 2006.

[4] M. G. Carmichael, S. Aldini, R. Khonasty, A. Tran, C. Reeks, D. Liu, K. J. Waldron, and G. Dissanayake, "The ANBOT: An Intelligent Robotic Co-worker for Industrial Abrasive Blasting," in *Proceedings of the 2019 IEEE International Conference on Intelligent Robots and Systems (IROS)*, 2019.

[5] S. Aldini, A. Akella, A. K. Singh, Y.-K. Wang, M. Carmichael, D. Liu, and C.-T. Lin, "Effect of Mechanical Resistance on Cognitive Conflict in Physical Human-Robot Collaboration," in *Proceedings of the 2019 IEEE International Conference on Robotics and Automation (ICRA)*, pp. 6137–6143, 2019.

[6] F. Rezazadegan, J. Geng, M. Ghirardi, G. Menga, S. Murè, G. Camuncoli, and M. Demichela, "Risked-based Design for the Physical Human-Robot Interaction (pHRI): an Overview," *Chemical Engineering Transactions*, vol. 43, pp. 1249–1254, 2015.

[7] D. Oetomo and M. H. Ang, "Singularity robust algorithm in serial manipulators," *Robotics and Computer-Integrated Manufacturing*, 2009.

[8] A. S. Deo and I. D. Walker, "Overview of damped least-squares methods for inverse kinematics of robot manipulators," *Journal of Intelligent & Robotic Systems*, 1995.

[9] B. Navarro, A. Fonte, P. Fraisse, G. Poisson, B. Navarro, A. Fonte, P. Fraisse, G. Poisson, A. Cherubini, and B. Navarro, "OpenPHRI : an open-source library for safe physical human-robot interaction," *Hal*, 2017.

[10] A. De Luca and F. Flacco, "Integrated control for pHRI: Collision avoidance, detection, reaction and collaboration," in *Proceedings of the IEEE RAS and EMBS International Conference on Biomedical Robotics and Biomechatronics*, 2012.

[11] P. Maurice, N. Hogan, and D. Sternad, "Predictability, force, and (anti)resonance in complex object control," *Journal of Neurophysiology*, 2018.

[12] M. S. Ryoo, "Human activity prediction: Early recognition of ongoing activities from streaming videos," in *Proceedings of the IEEE International Conference on Computer Vision*, 2011.

[13] S. J. Luck, "Event-Related Potentials," *APA Handbook of Research Methods in Psychology*, 2005.

[14] A. K. Singh, S. Aldini, D. Leong, Y.-K. Wang, M. G. Carmichael, D. Liu, and C.-T. Lin, "Prediction Error Negativity in Physical Human-Robot Collaboration," in *Proceedings of the IEEE 8th International Winter Conference on Brain-Computer Interface*, (Seoul, Korea), In Press, 2020.

[15] B. A. Francis and W. M. Wonham, "The internal model principle of control theory," *Automatica*, 1976.

[16] J. Cooper, *Cognitive dissonance: Fifty years of a classic theory*. 2007.

[17] M. Falkenstein, J. Hohnsbein, J. Hoormann, and L. Blanke, "Effects of crossmodal divided attention on late ERP components. II. Error processing in choice reaction tasks," *Electroencephalography and Clinical Neurophysiology*, 1991.

[18] A. K. Singh, H. T. Chen, Y. F. Cheng, J. T. King, L. W. Ko, K. Gramann, and C. T. Lin, "Visual Appearance Modulates Prediction Error in Virtual Reality," *IEEE Access*, 2018.

[19] K. Gramann, J. T. Gwin, D. P. Ferris, K. Oie, T. P. Jung, C. T. Lin, L. D. Liao, and S. Makeig, "Cognition in action: Imaging brain/body dynamics in mobile humans," *Reviews in the Neurosciences*, vol. 22, no. 6, 2011.

[20] I. Iturrate, L. Montesano, and J. Minguez, "Single trial recognition of error-related potentials during observation of robot operation," in *2010 Annual International Conference of the IEEE Engineering in Medicine and Biology Society, EMBC'10*, 2010.

[21] I. Iturrate, L. Montesano, and J. Mínguez, "Robot reinforcement learning using EEG-based reward signals," in *Proceedings - IEEE International Conference on Robotics and Automation*, 2010.

[22] C. I. Penaloza, Y. Mae, M. Kojima, and T. Arai, "Brain signal-based safety measure activation for robotic systems," *Advanced Robotics*, 2015.

[23] S. K. Ehrlich and G. Cheng, "Human-agent co-adaptation using error-related potentials," *Journal of neural engineering*, 2018.

[24] A. F. Salazar-Gomez, J. Delpreto, S. Gil, F. H. Guenther, and D. Rus, "Correcting robot mistakes in real time using EEG signals," in *Proceedings - IEEE International Conference on Robotics and Automation*, 2017.

[25] A. Puce and M. S. Hämäläinen, "A review of issues related to data acquisition and analysis in EEG/MEG studies," 2017.

[26] G. E. Chatrian, E. Lettich, and P. L. Nelson, "Ten percent electrode system for topographic studies of spontaneous and evoked EEG activity," *American Journal Of EEG Technology*, 1985.

[27] M. G. Carmichael and D. Liu, "Admittance control scheme for implementing model-based assistance-as-needed on a robot," in *Proceedings of the Annual International Conference of the IEEE Engineering in Medicine and Biology Society, EMBS*, 2013.

[28] A. Delorme and S. Makeig, "EEGLAB: An open source toolbox for analysis of single-trial EEG dynamics including independent component analysis," *Journal of Neuroscience Methods*, 2004.

[29] C. Y. Chang, S. H. Hsu, L. Pion-Tonachini, and T. P. Jung, "Evaluation of Artifact Subspace Reconstruction for Automatic EEG Artifact Removal," *Conference proceedings of the Annual International Conference of the IEEE Engineering in Medicine and Biology Society*, 2018.

[30] S. Makeig, A. J. Bell., T.-P. Jung, and T. J. Sejnowski, "Independent Component Analysis of Electroencephalographic Data," *Advances in Neural Information Processing Systems*, 1996.

[31] A. Mognon, J. Jovicich, L. Bruzzone, and M. Buiatti, "ADJUST: An automatic EEG artifact detector based on the joint use of spatial and temporal features," *Psychophysiology*, 2011.

[32] J. Polich, "Updating P300: An integrative theory of P3a and P3b," *Clinical Neurophysiology*, 2007.

[33] J. E. Trost, "Statistically nonrepresentative stratified sampling: A sampling technique for qualitative studies," *Qualitative Sociology*, 1986.

[34] International Federation of Clinical Neurophysiology, *Recommendations for the Practice of Clinical Neurophysiology: Guidelines of the International Federation of Clinical Physiology (EEG Suppl. 52)*. Elsevier Science B.V., 1999.

[35] E. Başar, C. Başar-Eroglu, S. Karakaş, and M. Schürmann, "Gamma, alpha, delta, and theta oscillations govern cognitive processes," *International Journal of Psychophysiology*, 2001.

[36] H. Zhang, A. J. Watrous, A. Patel, and J. Jacobs, "Theta and Alpha Oscillations Are Traveling Waves in the Human Neocortex," *Neuron*, 2018.

[37] F. Lotte, L. Bougrain, A. Cichocki, M. Clerc, M. Congedo, A. Rakotomamonjy, and F. Yger, "A review of classification algorithms for EEG-based brain-computer interfaces: A 10 year update," 2018.

[38] J. B. Yang, M. N. Nguyen, P. P. San, X. L. Li, and S. Krishnaswamy, "Deep convolutional neural networks on multichannel time series for human activity recognition," in *IJCAI International Joint Conference on Artificial Intelligence*, 2015.

[39] D. P. Kingma and J. L. Ba, "Adam: A method for stochastic gradient descent," *ICLR: International Conference on Learning Representations*, 2015.

[40] R. T. Schirrmeister, J. T. Springenberg, L. D. J. Fiederer, M. Glasstetter, K. Eggensperger, M. Tangermann, F. Hutter, W. Burgard, and T. Ball, "Deep learning with convolutional neural networks for EEG decoding and visualization," *Human Brain Mapping*, vol. 38, no. 11, 2017.

[41] C. M. Bishop, *Pattern Recogniton and Machine Learning*. 2006.